International Journal of Coal Geology 231 (2020) 103610

Contents lists available at ScienceDirect

International Journal of Coal Geology

journal homepage: www.elsevier.com/locate/coal

Critical metal recovery potential of Appalachian acid mine drainage treatment solids

Benjamin C. Hedin[a,b,*], Robert S. Hedin[b], Rosemary C. Capo[a], Brian W. Stewart[a]

[a] Department of Geology and Environmental Science, University of Pittsburgh, Pittsburgh, PA 15260, USA
[b] Hedin Environmental, Inc., 195 Castle Shannon Blvd., Pittsburgh, PA 15228, USA

ARTICLE INFO

Keywords:
Clean energy critical metals
Rare earth elements
Yttrium
Cobalt

ABSTRACT

Rare earth elements (REE) are critically important in clean energy technologies, but their mining and refining is energy intensive and generates significant quantities of environmentally harmful waste. The treatment of acid mine drainage (AMD), which is both a global environmental problem and a potential source of these elements, preconcentrates REE and critical metals such as manganese and cobalt into oxide/hydroxide waste products from which they can potentially be recovered. Analysis of 281 treatment solids from coal AMD remediation systems across the northern Appalachian Basin, eastern USA, indicate that the most promising solids (REE value > $400 USD/metric ton) are produced in systems that use limestone or sodium hydroxide to treat low pH (< 5) AMD with elevated dissolved aluminum and manganese content. In particular, recovering REE from passive treatment systems could both subsidize treatment of AMD while reducing the environmental footprint of REE extraction.

1. Introduction

The demand for metals such as Mn, Co, Ni, Ga, Cd, Ag, Cu, Se, In and rare earth elements (REE, defined here as the 15 lanthanide elements plus yttrium; DOE, 2011; Dominish et al., 2019) is expected to increase sharply in the coming decades due to their use in renewable energy technologies (e.g., wind turbines, electric motors, and batteries). However, sources of these elements are limited (Fishman and Graedel, 2019), and mining and refining these metals can have serious impacts on human health and the environment. For example, REE extraction from carbonatite and monazite ores produces large quantities of radioactive waste, uses significant amounts of energy, and is poorly regulated in some regions (Haque et al., 2014; Van Gosen et al., 2017). The need for both environmentally friendly and geographically diverse REE sources has spurred research into non-traditional feedstocks (Binnemans et al., 2013; Hein et al., 2013; Lin et al., 2018; Stuckman et al., 2018; Takaya et al., 2018), including polluted mine drainage (Ayora et al., 2016; Hedin et al., 2019; Lefticariu et al., 2019; Stewart et al., 2017; Vass et al., 2019b).

Oxidation and dissolution of sulfide minerals (e.g., pyrite, FeS_2) related to coal and metal mining produces acidity and dissolved metals that pollute waterways around the world with acid mine drainage (AMD; Younger et al., 2002). In the Appalachian basin in the eastern USA, over two centuries of coal mining has produced thousands of pollution sources that impair over 5000 km of streams with acidity, metals, and sulfate (EPA, 2015). However, Appalachian AMD also generates between 500 and 3400 metric tons of REE annually, depending on estimates of total AMD discharge and REE concentrations (Stewart et al., 2017; Vass et al., 2019a). This represents 7% - 41% of annual US consumption of REE in 2018 (Gambogi, 2019a, 2019b). Total REE loads for single AMD discharges can be up to 7000 kg/year, with many discharges producing greater than 100 kg/year (Cravotta, 2008a; Cravotta and Brady, 2015; Stewart et al., 2017).

AMD treatment involves pH and redox adjustments to neutralize acidity and accelerate the precipitation and settling of dissolved metals (Younger et al., 2002). This generates significant amounts of solid waste; more than 18,000 metric tons are produced annually in Pennsylvania alone (Stream Restoration, 2018). The management and disposal of these treatment solids incur significant costs to operators (Cravotta et al., 2014). With REE concentrations reported as high as 2000 mg/kg, these solids could be targeted for REE recovery, and could offset the cost of treating AMD (Hedin et al., 2019; Vass et al., 2019b).

Although there has been substantial work on identifying and characterizing REE-enriched AMD treatment solids, most estimates are based on relatively small sample sizes (< 25), or are limited to a few sites and do not focus on geochemical trends of solids associated with AMD chemistry or treatment technology (Acero et al., 2006; Hedin et al., 2019; Lozano et al., 2019a, 2020; Lozano et al., 2019b; Moraes

* Corresponding author at: Department of Geology and Environmental Science, University of Pittsburgh, Pittsburgh, PA 15260, USA.
E-mail address: BCH37@pitt.edu (B.C. Hedin).

https://doi.org/10.1016/j.coal.2020.103610
Received 15 June 2020; Received in revised form 21 September 2020; Accepted 3 October 2020
Available online 06 October 2020

et al., 2020; Stewart et al., 2017; Vass et al., 2019a, 2019b). Additionally, there is limited work on the potential to recover other clean energy critical elements (Mn, Co, Ni, Ga, Cd, Ag, Cu, Se) from treatment solids. In this study, we report major and trace element concentrations for 281 AMD precipitates from 94 sites across the Appalachian Basin, with corresponding untreated AMD pH and treatment technology information to determine (1) the relationship between AMD chemistry and clean energy critical metal concentrations in treatment solids, (2) the impact of treatment technology on REE concentrations and geochemical trends, and (3) potential REE market value in AMD treatment solids. While we focus on REE in AMD treatment solids, we also report on the concentrations and geochemical trends for other clean energy critical metals. These results can be used to identify promising feedstocks from existing treatment systems and inform the design of new systems optimized to both remediate polluted water and concentrate economic amounts of critical metals in treatment solids.

2. Materials and methods

2.1. Data sources

Treatment solids chemistry and AMD water chemistry used in this study include both published and previously unpublished data (Table 1). Solids chemistry for 281 samples is compiled from Hedin et al., 2019 (n = 11), Stewart et al., 2017 (n = 21) and unpublished data from Hedin Environmental (n = 249). For 170 samples, total REE concentrations are calculated from Y concentrations based on a robust linear regression (see details in section 2.2). Paired AMD water chemistry is compiled for 225 samples from Beam, 2019 (n = 2), Cravotta and Brady, 2015 (n = 2), Cravotta, 2008a (n = 33), Hedin et al., 2019 (n = 13), Stewart et al., 2017 (n = 12), www.datashed.org (Stream Restoration, 2018; an online AMD chemistry data repository; n = 23), and unpublished data from Hedin Environmental (n = 140). Treatment technology for 251 samples is compiled from Hedin Environmental.

2.2. Treatment solids chemistry

Treatment solids analyzed for this study were grab samples from either AMD treatment systems or naturally attenuated (untreated) locations and were collected by shovel or bucket. Samples were dried at 100 °C until weight was constant. If limestone aggregate was collected, it was sieved to 2 mm after drying to separate treatment solids (< 2 mm) from the aggregate (> 2 mm). AMD pH was measured by calibrated pH meters in the field.

The treatment solid samples collected in this study were analyzed by Activation Laboratories Ltd. (accredited by the Canadian Association for Laboratory Accreditation) by ICP-MS and/or ICP-OES. When these samples were combined with literature data from Hedin et al. (2019) and Stewart et al. (2017), thirteen of the samples have all REE concentrations (Y + lanthanides) measured by ICP-MS (Table 2). For 35 samples with concentrations for 9 out of 15 REE (Y, La, Ce, Na, Sm, Eu, Tb, Yb, Lu) measured by instrumental neutron activation analysis (INAA), missing REE concentrations were interpolated as the weighted average between the two nearest redox-insensitive REE_{NASC} ratios for calculation of total REE concentrations (see Table S1 and S2 for equations and justification). For 45 samples, concentrations of between 2 and 8 of the REE are above detection limits, and 170 samples have only Y concentrations measured by ICP-OES or ICP-MS (Table 2). Because the relationship between Y and total REE concentrations is robust (r^2 = 0.88; p < 0.001; Fig. 1) and Y and lanthanides behave similarly (Bau and Dulski, 1996), total REE concentrations were estimated for these 215 samples as follows:

$$Total\ REE\ (ppm) = Y\ (ppm) \times 4.1063$$

The regression between Y and total REE concentrations is nearly identical for samples with REE only measured by ICP-MS versus using the methods described above (Fig. 1).

Samples were further classified into Al- and Mn-rich (> 10% Al + Mn) and Fe-rich (> 10% Fe and < 10% Al + Mn) to determine if major element composition impacts the Y and REE relationship. While the slopes of the regressions are slightly different (4.19 for Al- and Mn-rich and 3.36 for Fe-rich; Fig. S1), the linear regression using all data (Fig. 1) is appropriate to calculate total REE concentrations from Y for the entire dataset.

2.3. Stepwise regression

Multivariate linear regressions constructed using stepwise linear regression to assess co-associations between REE, critical metals, and associated mineralogy can inform the search for valuable AMD

Table 1
Data sources for this study and number of samples from each source. Datashed is an online AMD chemistry data repository (Stream Restoration, 2018).

Treatment solids	n	AMD liquid	n	Treatment technology	n
Hedin et al., 2019	11	Beam, 2019	2	This study	251
Stewart et al., 2017	21	Cravotta and Brady, 2015	2		
This study	249	Cravotta, 2008a	33		
		Hedin et al., 2019	13		
		Stewart et al., 2017	12		
		www.datashed.org	23		
		This study	140		
Total	281		225		251

Table 2
Appalachian AMD treatment solid samples and analyses included in this database.

REE concentrations above detection limits	Number of samples	Analysis
Total REE (Y + all lanthanides)	13	Correlate total REE with Y
Full INAA analysis (Y, La, Ce, Nd, Sm, Eu, Tb, Yb, Lu)	35	Calculate missing REE via Table S2 and correlate with Y
Partial REE (> 1 REE, < 9 REE)	45	Calculate total REE using Y
Y only	170	Calculate total REE using Y
All REE below detect	18	Unused

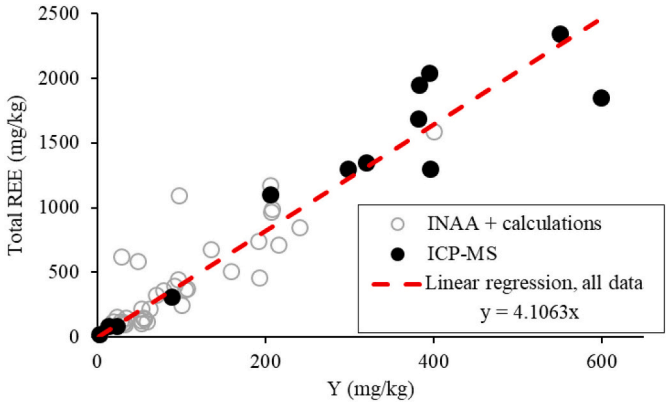

Fig. 1. Linear regression between Y and total REE concentrations (both ICP-MS and INNA + calculations; r^2 = 0.88, p < 0.001). The regression with only ICP-MS measured data is y = 4.1022×; r^2 = 0.88. Sample analyzed using ICP-MS have all 15 REE measured. Samples analyzed using INAA points have 9 REE measured (Y, La, Ce, Nd, Sm, Eu, Tb, Yb, Lu) and remaining REE concentrations are calculated as detailed in methods.

treatment solids. Independent variables chosen for this analysis were concentrations of Si, Al, Fe, Mn, Mg, Ca, and LOI (loss on ignition; includes volatile components such as H_2O and CO_2 from hydrated minerals, carbonate, and/or organic matter). Clean energy-critical elements considered as dependent variables were REE, Co, Ni, Cu, Ga, Cd, and Ag.

Only samples for which the sum of Si, Al, Fe, Mn, Mg, Ca oxides and LOI was greater than 90% were used in the regression; this requirement excluded three samples out of 281. The stepwise regression function in Matlab 2019a was used to generate multivariate linear regressions that maximizes explanatory power. The inclusion/exclusion of independent variables is determined by calculating p values for the models with and without an independent variable. If the weight of the variable is significantly statistically different from zero ($p < 0.05$), it is added to the model.

2.4. Economic evaluation

In-situ and basket REE prices were calculated based on average prices from the 2008 to 2015 USGS Mineral Yearbooks following the methodology of Vass et al. (2019a) for 48 treatment solid samples with complete REE concentrations, and for 58 REE mineral resources that are currently under development (Lifton and Hatch, 2015). In situ prices for Co were calculated using the average yearly London Metal Exchange price of Co from 2015 to 2019 ($42.98/kg; US Department of the Interior, 2020).

3. Results and discussion

3.1. Characteristics of AMD treatment solids

Complete data from the 281 treatment solid samples from 94 AMD treatment systems in northern Appalachia are presented in Supplementary Table 4. A similar database with 629 treatment solid samples from 119 sites across Appalachia was compiled by West Virginia University and is freely available through the US Department of Energy's National Energy Technology Laboratory Energy Data eXchange (National Energy Technology Laboratory, 2018). Although this database is extensive, it does not report Mn or volatiles, which can be substantial components of treatment solids, and the only trace metals reported are REE and Co. Thus, only the 281 samples compiled in this study are used in this analysis.

Major constituents in Appalachian AMD treatment solids include Al, Fe, Mn, Ca, Mg and Si. This is reflected in the mineralogy of the solids, which generally includes Al-, Fe-, Mn-, Ca-, and Mg-hydrated oxides and hydroxides, Ca and Mg carbonates and/or hydroxides, gypsum, and silica (Cravotta and Trahan, 1999; Kairies et al., 2005; Pu et al., 2010; Tan et al., 2010). XRD analysis indicates many of these solids are amorphous or poorly-crystalline (Cravotta and Trahan, 1999; Hedin et al., 2019; Kairies et al., 2005; Pu et al., 2010). Percentile concentrations of critical metals are provided in Table 3. Manganese (Mn), a major metal pollutant in Appalachian AMD, was as high as 43% in the solids with two samples above the average global sedimentary Mn ore deposit value of 24% (Cannon et al., 2018). The two highest Co concentrations (5050 mg/kg and 2940 mg/kg) were comparable to low grade Co ores (2000–10,000 mg/kg; Slack et al., 2017). Additionally, Co concentrations in six samples were above laboratory reporting limits (1000 mg/kg). Among other critical metal resources, Ni (≤ 6800 mg/kg) and Cu (≤ 740 mg/kg) are below traditional laterite (8300–18,000 mg/kg; Berger et al., 2011) and porphyry (1000–16,000 mg/kg; Singer et al., 2008) sources, respectively. Gallium concentrations (≤ 17 mg/kg) are equivalent to or lower than continental crust concentrations (17–18 mg/kg; Foley et al., 2017). Both Cd (≤ 13 mg/kg) and Ag (≤ 4.4 mg/kg) are already recovered as byproducts from refining Zn and Zn/Pb ores, respectively (Goonan, 2014; Shiel et al., 2010). All In and Se measurements were at or below detection limits (0.2 mg/kg and 3 mg/kg, respectively).

Table 3
The range in critical metal concentrations for AMD treatment solids. Percentile data were calculated from samples with concentrations above detection limits.

Percentile	REE	Mn	Co[a]	Ni	Cu	Ga	Cd	Ag
	mg/kg							
100 (maximum)	2344	427,497	5050	6720	731	17	13.1	4.4
75	255	2168	94	355	57	15	2.0	0.7
50	115	620	14	32	17	13	1.7	0.5
25	61	232	5	14	9	6	1.3	0.5
0 (minimum)	4	100	1	4	1	4	0.5	0.3
# analyses	261	278	98	82	82	11	74	82
Minimum detection limit (mg/kg)	1	100	1	1	1	1	0.5	0.5
# below detection	0	1	5	0	15	0	7	60

[a] Six samples have greater than 1000 mg/kg Co.

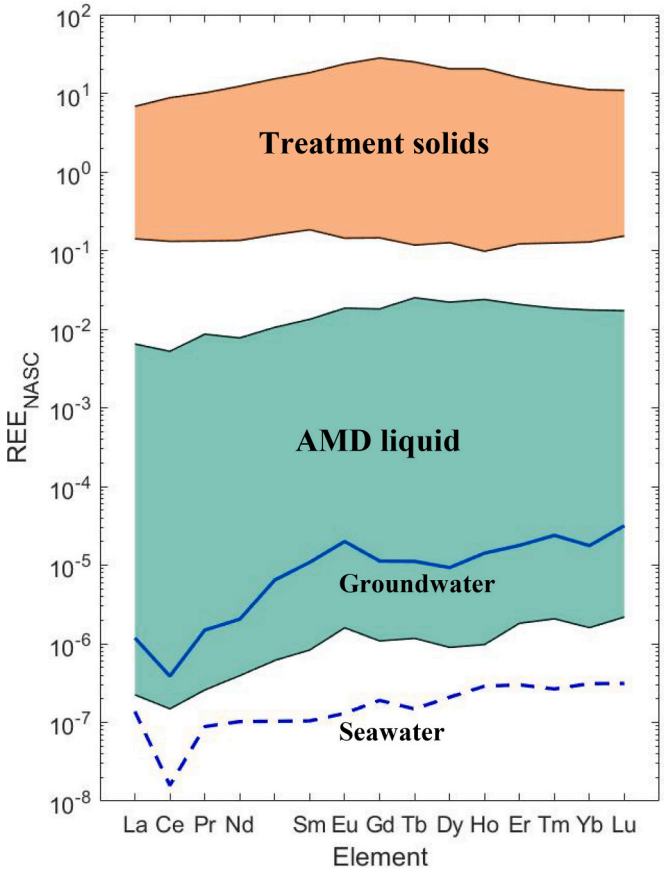

Fig. 2. North American Shale Composite normalized REE patterns for the seawater and groundwater samples with median total REE concentrations (Noack et al., 2014), AMD liquid samples with the highest and lowest total REE concentrations (Cravotta, 2008b; Cravotta and Brady, 2015; Hedin et al., 2019; Stewart et al., 2017), and treatment solids with the highest and lowest total REE concentrations from this study. Y is not included in this plot.

Although untreated AMD has a higher REE content than natural waters, treatment solids are enriched by several orders of magnitude relative to either (Fig. 2). Total REE concentrations in treatment solids range from 4 to ~2300 mg/kg (Table 3). The highest concentrations of REE are associated with solids with substantial Al, and Mn content (Fig. 3). While the REE concentrations in these enriched samples are well below the concentrations in carbonatite and monazite REE ores (30,000 mg/kg to 80,000 mg/kg), they are similar to concentrations in ion-absorbed clay deposits in Southern China (500 mg/kg to 4000 mg/

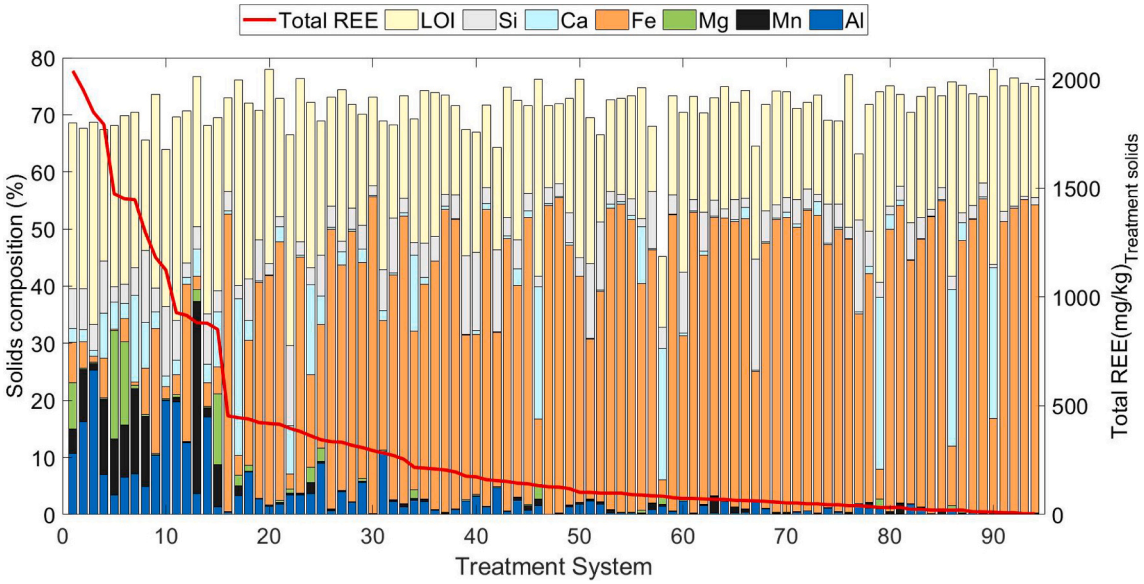

Fig. 3. Average AMD treatment solids content and total REE concentrations from 94 treatment systems or naturally attenuated sites across northern Appalachia.

kg; Van Gosen et al., 2017). Ion absorbed clay REE deposits in South China are economical to exploit, in part, because of their high proportion of high-value heavy REE (Tb, Dy, Y, Ho, Er, Tm, Yb, Lu); they contain about 80 wt%, compared to under 2 wt% for carbonatite/monazite ores (Bao and Zhao, 2008; Castor, 2008; Lynas Corporation Ltd, 2012). Treatment solids are similarly enriched in heavy REE (average 49 wt%; Hedin et al., 2019; Stewart et al., 2017).

Treatment solids also contain a high proportion of green energy technology-critical REE (Y, Nd, Dy, Eu, and Tb; DOE, 2011). Total concentrations of critical REE range from 7 mg/kg to ~1000 mg/kg and make up 27% to 67% of total REE concentrations in the solids (Fig. S2); Yttrium and Nd alone make up 26 ± 10% and 16 ± 4% of total REE concentrations, respectively. The proportion of green energy-critical REE in treatment solids are comparable to other unconventional REE feedstocks currently under consideration, such as coal fly ash, deep sea muds, and ocean Fe–Mn nodules (Bau et al., 2014; Stuckman et al., 2018; Takaya et al., 2018), and approaches that of ion-absorbed REE clays (76%) in China (Bao and Zhao, 2008). Additionally, concentrations of U and Th in carbonatite and monazite REE ores can be up to 400 mg/kg (Castor, 2008) and present an environmental challenge due to their radioactivity when processing these ores. AMD precipitates are significantly lower in U (5.8 ± 5.9 mg/kg; max. 26 mg/kg) and Th (4.3 ± 7.2 mg/kg; max. 51 mg/kg; Fig. S3).

These data suggest that while treatment solids can be enriched in Mn and Co, there are very few samples in this database with concentrations comparable to ores. However, REE concentrations are comparable to currently exploited ores and could be prioritized for recovery from AMD treatment solids.

3.2. Geochemical relationships

The multivariate linear regressions are shown in Table 4 and have strong prediction power ($r^2 > 0.60$) for REE, Co, Ni, Ga, and Ag. For REE, the multivariate linear regression indicates that treatment solids with high concentrations of Al, Mn, and Mg (positive weights) are likely to have high concentrations of REE, while those with high Si and LOI concentrations are likely to have low concentrations of REE (negative weights). Likewise, higher Mn and Al concentrations are also associated with higher concentrations of Co. However, for Co, Mn is an order of magnitude more important than Al and dominates the multivariate regression.

Previous work on REE in AMD treatment solids shows that REE are associated with Al rich solids (Ayora et al., 2016; Lozano et al., 2019a; Lozano et al., 2019b; Moraes et al., 2020). However, Table 4 shows that solids with high concentrations of Mn and Mg can also have high concentrations of REE. Furthermore, Fig. 3 shows that REE enriched solids are typically geochemically complex, containing Al, Mn, Fe, and Mg minerals. This is significant because the presence of a diverse mineralogical assemblage suggests complex REE attenuation mechanisms (e.g., sorption on Fe, Al, and Mn oxides and hydroxides) are possible and that both Al- and Mn-rich solids are important to consider when targeting treatment solids for REE recovery.

Table 4
Results of the stepwise linear regression where major element concentrations (%) are used as independent variables to calculate critical metal concentrations (mg/kg).

Variables	REE	Co	Ni	Cu	Ga	Cd	Ag
	Weights						
y intercept	234	0.9	1.6	8.9	17.2	1.84	0.51
Si (%)	−12[c]	−9.3	−21.4	−2.3	0.2	−0.05	0.00
Al (%)	65[c]	18.6[b]	25.4[a]	12.0[c]	−0.4[b]	0.01	0.02
Fe (%)	−3	−3.8	−3.4	−0.9	−0.2	−0.01	0.00
Mn (%)	40[c]	180.4[c]	179.2[c]	2.4	0.1	0.28[c]	0.16[c]
Mg (%)	43[c]	−50.4[a]	−33.3	−6.7	−1.4[b]	−0.37[b]	−0.01
Ca (%)	2	7.8	11.2	1.7	0.0	0.04	−0.01[a]
LOI (%)	−7[b]	4.6	2.5	3.0	−0.1	0.01	−0.01
Regression r^2	0.70	0.76	0.63	0.33	0.77	0.32	0.99

[a] $p < 0.05$.
[b] $p < 0.01$.
[c] $p < 0.001$

Cobalt is strongly co-associated with Mn in AMD treatment solids in this study, as is common in ocean and freshwater systems (Lienemann et al., 1997). Although Co and Al are positively correlated, some samples with high Al concentrations have low Co concentrations (Fig. S4). Additionally, the six samples with greater than 1000 mg/kg Co all contain at least 91,000 mg/kg Mn.

Although organic matter has strong REE chelating abilities (Tanizaki et al., 1992), LOI is negatively weighted in the REE linear regression and is not well correlated with total REE concentrations ($r^2 = 0.12$). Similarly, while dissolved Si concentrations are highest in low pH AMD (Cravotta, 2008a), Si and total REE concentrations are poorly correlated ($r^2 = 0.01$). This suggests that Si and LOI dilute, rather than concentrate, REE in treatment solids.

3.3. Optimizing REE recovery in treatment solids

Trace metal content and statistical analyses indicate that AMD treatment solids with high Al and Mn concentrations should be targeted for recovery of REE and Co. Additionally, multiple samples collected from single treatment sites indicate that there is low intra-site variability in REE concentrations compared to variability between sites, which suggests that potential REE resource recovery for individual sites could be adequately determined by analyzing a few samples (Fig. S5). Although REE may be uniquely partitioned between solid phases (e.g., preferentially adsorbed onto specific metal oxides), bulk geochemical relationships can inform the identification of treatment solids amenable for REE recovery.

3.3.1. Iron-rich precipitates

While iron oxide can be a strong sorbent of REE and Co (Dzombak and Morel, 1990; Verplanck et al., 2004), Fe in AMD treatment solids is negatively correlated with REE ($r^2 = 0.31$, $p < 0.01$) and Co ($r^2 = 0.17$, $p < 0.01$), and iron-rich treatment solids typically contain low total REE and Co concentrations (Fig. 3, Fig. S4). The reasons for this relate to pH-based treatment of coal mine discharges. Minewaters that are both anoxic (dissolved oxygen < 1 mg/L) and circumneutral (pH ~7) are a common occurrence in Appalachia (Cravotta, 2008a). Under these conditions, Fe(II) is soluble while Al, REE, and Co are minimally soluble and/or are not leached from associated strata. Treatment of this type of mine drainage oxidizes and precipitates Fe, resulting in Fe-rich solids with low REE and Co concentrations. Treatment of low pH, high Fe minewaters solely by microbial Fe(II) oxidation also results in solids with high Fe and low REE and Co concentrations (Hedin et al., 2019).

3.3.2. Al- and Mn-rich precipitates

Rare earth element, Co, Al, and Mn concentrations are highest in low pH discharges because these elements are leached from rock units by acidic minewater (Cravotta, 2008a; Wallrich et al., 2020). By neutralizing acidity and raising pH, dissolved metals can be precipitated. At pH 6–9, Al is minimally soluble and precipitates (Cravotta, 2008b); dissolved REE are also removed from solution by adsorption on Fe, Al and/or Mn oxide/hydroxides surfaces and/or co-precipitation with these metals (Ayora et al., 2016; Hedin et al., 2019; Lozano et al., 2019b; Verplanck et al., 2004). Likewise, dissolved Co is removed from solution by adsorption on Fe/Mn oxide/hydroxide surfaces followed by substitution into Mn oxide structures (Burns, 1976; Lienemann et al., 1997). Manganese can be removed at pH greater than 9 by stoichiometric solubility controls (Cravotta, 2008b) or at pH 6–7 by heterogeneous precipitation on biogenic Mn coatings on limestone (Santelli et al., 2011; Tan et al., 2010).

3.3.3. Treatment technology

To determine which AMD treatment systems should be prioritized for REE recovery, current treatment technology must also be considered. Because of the pH dependency of REE concentrations in AMD, solids from systems treating AMD with pH greater than 5 typically contain total REE less than 500 mg/kg, and solids from AMD with pH less than 5 can have REE concentrations from less than 500 mg/kg to greater than 2000 mg/kg (Fig. 4). The impact of chemistry and treatment technology described below for REE likely also explain the variability and geochemical relationships for other clean energy critical metals and can inform their recovery from treatment solids.

The wide range in total REE concentrations in treatment solids produced from pH less than 5 AMD is explained by the variety of acid neutralization technologies used in treatment. Typical active treatment technologies (in which chemicals are mixed with AMD in reaction tanks) utilized to neutralize acidity are sodium hydroxide (NaOH) or lime (either $Ca(OH)_2$ or CaO). In passive treatment systems limestone (consisting of calcite, $CaCO_3$) is usually used to neutralize acidity.

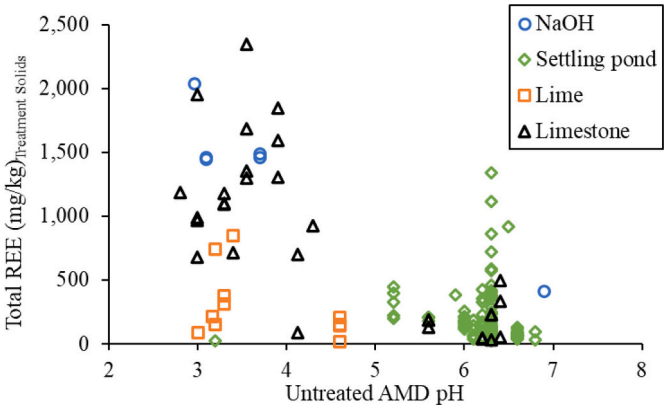

Fig. 4. Paired untreated AMD pH and total REE concentrations in the treatment solids for 185 samples from 44 treatment systems using NaOH, lime, limestone, and settling ponds.

Systems using lime to neutralize acidity typically produce treatment solids with lower total REE concentrations (283 ± 258 mg/kg; one standard deviation) than systems using limestone or sodium hydroxide (1211 ± 522 mg/kg and 1578 ± 258 mg/kg, respectively; Fig. S6). Higher average Ca concentrations in lime solids (19% ± 9%) compared to those from limestone and sodium hydroxide systems (3–6%) suggest that the lower REE concentrations are due to dilution by calcite and unreacted lime. Calcite commonly precipitates after the addition of lime because of high pCO_2 in minewaters (Cravotta, 2008a). However, modern hydrated lime treatment systems with CO_2 degassing technology and pH-controlled lime dosing can produce solids with low Ca content (5% Ca; Beam, 2019) which could then potentially increase relative REE content.

Treatment solids produced from pH less than 5 AMD using sodium hydroxide to neutralize acidity produce solids with high REE. However, Mg concentrations are also high (15% ± 4%) compared to the Mg content of solids from limestone and lime systems (< 1–3%). High Mg concentrations are a result of raising pH above 9 to precipitate Mn as MnO_2 and/or MnOOH. Magnesium, also minimally soluble in this pH range, will precipitate as $Mg(OH)_2$ together with Mn and REE, as observed in the REE multivariate regression (Table 4).

Treatment solids produced from pH less than 5 AMD using limestone to neutralize acidity typically produce solids with high REE concentrations and low Ca and Mg concentrations (< 6%). The bicarbonate buffering range of limestone dissolution minimizes the solubility of Al and Fe, promotes heterogeneous Mn removal, and minimizes Ca and Mg precipitation. A common maintenance task for passive treatment systems is the use of pumps and excavators to wash treatment solids from limestone beds. This produces segregated solids primarily composed of Al, Mn, Fe, and Si. For these reasons, limestone-based systems produce the treatment solids with both high REE concentrations and low non-target metal concentrations (e.g., Ca, Mg).

Limestone treatment systems also produce solids with the highest concentrations of Co. All nine samples with Co concentrations greater than 1000 mg/kg are from limestone systems. Hedin et al., 2019 showed that Mn rich coatings that form on limestone aggregate can contain high concentrations of Co (> 5000 mg/kg).

3.4. REE and Co resources in appalachian AMD

In situ and basket REE prices can be used to evaluate and compare potential REE sources (Silva et al., 2018) and can be applied to AMD treatment solids (Vass et al., 2019a). In situ price refers to the REE value in one metric ton of raw material (dry weight); basket price is the REE value in 1 kg of pure REE product, assuming 100% REE can be extracted from the raw material. Because each REE is valued differently, in situ prices depend on REE distribution and concentration and

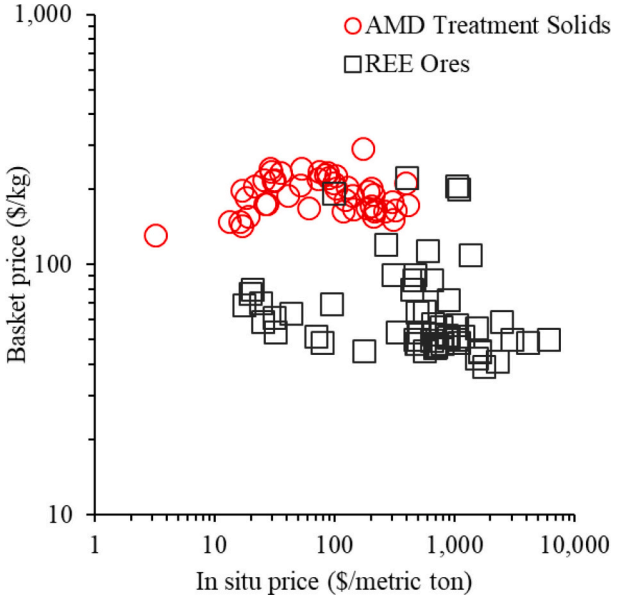

Fig. 5. In-situ and basket REE prices of Appalachian AMD treatment solids and developed/developing REE ores from around the world (Lifton and Hatch, 2015).

basket prices depend only on REE distribution.

In-situ prices (in $USD) of Appalachian AMD treatment solids range from $3/metric ton to $405/metric ton; basket prices range from $131/kg to $292/kg (Fig. 5). In-situ and basket prices of REE ores range from $18/metric to $6023/metric ton and from $39/kg to $213/kg, respectively (Lifton and Hatch, 2015).

Although in-situ and basket prices for treatment solids and REE ores are highly variable, there is significant overlap. REE concentrations in treatment solids range from 4 mg/kg to 2460 mg/kg whereas REE concentrations in ores range from 256 mg/kg to 120,000 mg/kg (12%). However, REE in treatment solids are in a metal hydroxide/oxide matrix that is potentially easier to process than traditional sources which are mostly hosted in silicate or carbonatite igneous rocks (Van Gosen et al., 2017). Additionally, AMD treatment solids contain low concentrations of U and Th, radioactive elements of concern in many REE ores.

In addition, basket REE prices for treatment solids are two to three times greater than those for REE ores. This is because AMD treatment solids contain a higher proportion of heavy REE (HREE) which are more valuable than light REE (LREE; La, Ce, Pr, Nd, Sm, Eu, Gd). The average HREE/LREE ratios for treatment solids and REE ores are 0.74 (± 0.43) and 0.19 (± 0.47), respectively. The small range in treatment solid basket prices for the treatment solids is due to their relatively homogeneous source (Pennsylvanian age sedimentary rocks in the Appalachian basin), compared to global REE ores.

Estimated Co in situ prices range from $0.04/metric ton to $217/metric ton. However, most solids (n = 73; 84%) would be valued at under $10/metric ton and only two are over $100/metric ton. Treatment solids with more economic concentrations of Co (> 2000 mg/kg) are associated with solids with high Mn concentrations (> 30%). While in situ prices are only one variable in determining the viability of resource extraction and market prices are volatile, the value of clean energy critical metals in AMD solids is driven by REE.

3.5. Treatment costs and sustainability

While currently operating AMD systems offer a potentially inexpensive source of REE-enriched solids, the cost and sustainability of AMD treatment are critical factors for future AMD treatment systems engineered for REE recovery. In Appalachia, the cost of using limestone as a neutralization agent is less than 20% of the cost of hydrated lime and sodium hydroxide (Cravotta et al., 2014). Limestone is also inert, compared to caustic sodium hydroxide, and has a lower CO_2 footprint compared to lime which requires the energy-intensive process of limestone calcination (Bosoaga et al., 2009). In addition, in order to produce low-Ca solids, the construction of modern lime treatment systems typically cost $10 to $15 million USD with hundreds of thousands of dollars per year in operation and maintenance (Beam, 2019).

An additional sustainability concern is the amount and nature of chemicals used in the processing of treatment solids. In many REE processing chains, the use of mineral acids (e.g., HCl) to solubilize REE accounts for about 40% of the greenhouse gas emissions in the REE processing chain (Haque et al., 2014). Treatment solids from lime and sodium hydroxide systems can contain high concentrations of Ca and Mg hydroxides/carbonates which would need to be dissolved before REE are solubilized at low pH. Treatment solids physically removed from limestone aggregate would require less acid to solubilize REE than other methods.

Although cheaper, the use of limestone to treat large flows of severely contaminated AMD requires more land than lime or sodium hydroxide technologies and additional considerations to maintain porosity and reactivity compared to lime or sodium hydroxide (Skousen et al., 2017). Despite these challenges, the effective treatment of severe AMD with limestone-based technologies has been demonstrated in both large and small scale systems (Caraballo et al., 2009; Hedin et al., 2010) that can serve as models to leverage the high REE concentrating efficiency, low cost, and sustainability of limestone to provide the best technology for recovering REE from AMD.

4. Conclusions

Although Mn and Co are substantially enriched in some treatment solids, REE (including Y) appear to be the most promising clean energy critical metals to recover from waste AMD treatment solids. Recovering REE from these solids offers a more sustainable source of REE compared to many traditional and non-traditional sources by (1) eliminating mining impacts, (2) generating lower U and Th content, and (3) reduced use of chemicals needed for processing. Total REE concentrations in solids currently produced from AMD treatment systems across Appalachia can contain over 2000 mg/kg dry weight and the variability in REE in AMD treatment solids can be predicted by AMD pH and the neutralization technology used in the remediation system. The highest total REE concentrations are associated with solids containing high Al and Mn concentrations. Geochemical relationships indicate that REE recovery will be maximized in systems that treat low pH (< 5) and high Al and/or Mn- containing AMD, using methods such as limestone treatment that can minimize nontarget solids precipitation.

For future systems designed to treat AMD and concentrate REE into solids, the use of limestone as an acid neutralization agent should be considered because it is significantly less costly than lime or sodium hydroxide, has a lower environmental footprint, and produces solids with high REE concentrations. The value of REE in treatment solids, up to $405 USD/metric ton of dry material, could offset the treatment costs of AMD that pollutes many surface waters worldwide. The framework developed here can help in the identification of promising REE and critical metal sources, evaluation of the economics of REE capture, and in engineering treatment systems to maximize REE recovery in solids, thus transforming an economic and environmental liability into a valuable resource.

Declaration of Competing Interest

The authors declare that they have no known competing financial interests or personal relationships that could have appeared to influence the work reported in this paper.

Acknowledgements

This research was supported by a University of Pittsburgh Mellon Predoctoral Fellowship (BCH), and a University of Pittsburgh Central Research Development grant (RCC), with technical support and data from Hedin Environmental. We appreciate the help with statistical analysis from Dr. Eitan Shelef at the University of Pittsburgh.

Appendix A. Supplementary data

Supplementary data to this article can be found online at https://doi.org/10.1016/j.coal.2020.103610.

References

Acero, P., Ayora, C., Torrentó, C., Nieto, J.-M., 2006. The behavior of trace elements during schwertmannite precipitation and subsequent transformation into goethite and jarosite. Geochim. Cosmochim. Acta 70, 4130–4139.
Ayora, C., Macias, F., Torres, E., Lozano, A., Carrero, S., Nieto, J.M., Perez-Lopez, R., Fernandez-Martinez, A., Castillo-Michel, H., 2016. Recovery of rare earth elements and yttrium from passive-remediation systems of acid mine drainage. Environ. Sci. Technol. 50, 8255–8262.
Bao, Z., Zhao, Z., 2008. Geochemistry of mineralization with exchangeable REY in the weathering crusts of granitic rocks in South China. Ore Geol. Rev. 33, 519–535.
Bau, M., Dulski, P., 1996. Distribution of yttrium and rare-earth elements in the Penge and Kuruman iron-formations, Transvaal Supergroup, South Africa. Precambrian Res. 79, 37–55.
Bau, M., Schmidt, K., Koschinsky, A., Hein, J., Kuhn, T., Usui, A., 2014. Discriminating between different genetic types of marine ferro-manganese crusts and nodules based on rare earth elements and yttrium. Chem. Geol. 381, 1–9.
Beam, R.L., 2019. Overview of Acitive Mine Drainage Treatment Facilities Currently Operated by the PA-DEP Bureau of Abandoned Mine Reclamation, West Virginia Mine Drainage Task Force Symposium, Morgantown, WV.
Berger, V.I., Singer, D.A., Bliss, J.D., Moring, B.C., 2011. Ni-Co laterite deposits of the world - database and grade and tonnage models. In: U.S. Geological Survey Open-File Report 2011-1058, pp. 1–30.
Binnemans, K., Jones, P.T., Blanpain, B., Van Gerven, T., Yang, Y., Walton, A., Buchert, M., 2013. Recycling of rare earths: a critical review. J. Clean. Prod. 51, 1–22.
Bosoaga, A., Masek, O., Oakey, J.E., 2009. CO2 capture technologies for cement industry. Energy Procedia 1, 133–140.
Burns, R.G., 1976. The uptake of cobalt into ferromanganese nodules, soils, and synthetic manganese (IV) oxides. Geochem. Cosmochim. Acta 40, 95–102.
Cannon, W.F., Kimball, B.E., Corathers, L.A., 2018. Manganese, Chapter L of Critical Metal Resources of the United States - Economic and Environmental Geology and Prospects for Future Supple. U.S. Geological Survey Professional Paper 1802. pp. L1–L28.
Caraballo, M.A., Rötting, T.S., Macías, F., Nieto, J.M., Ayora, C., 2009. Field multi-step limestone and MgO passive system to treat acid mine drainage with high metal concentrations. Appl. Geochem. 24, 2301–2311.
Castor, S.B., 2008. The mountain pass rare-earth carbonatite and associated ultrapotassic rocks, California. Can. Mineral. 46, 779–806.
Cravotta, C.A., 2008a. Dissolved metals and associated constituents in abandoned coal-mine discharges, Pennsylvania, USA. Part 1: Constituent quantities and correlations. Appl. Geochem. 23, 166–202.
Cravotta, C.A., 2008b. Dissolved metals and associated constituents in abandoned coal-mine discharges, Pennsylvania, USA. Part 2: Geochemical controls on constituent concentrations. Appl. Geochem. 23, 203–226.
Cravotta, C.A., Brady, K.B.C., 2015. Priority pollutants and associated constituents in untreated and treated discharges from coal mining or processing facilities in Pennsylvania, USA. Appl. Geochem. 62, 108–130.
Cravotta, C.A., Trahan, M.K., 1999. Limestone drains to increase pH and remove dissolved metals from acidic mine drainage. Appl. Geochem. 14, 581–606.
Cravotta, C.A., Means, B.P., Arthur, W., McKenzie, R.M., Parkhurst, D.L., 2014. AMDTreat 5.0+ with PHREEQC titration module to compute caustic chemical quantity, effluent quality, and sludge volume. Mine Water Environ. 34, 136–152.
DOE, 2011. U.S. Department of Energy Critical Materials Strategy.
Dominish, E., Florin, N., Teske, S., 2019. Responsible Minerals Sourcing for Renewable Energy. (Report prepared for Earthworks by the Institute for Sustainable Futures).
Dzombak, D.A., Morel, F.A.A., 1990. Surface Complexation Modeling: Hydrous Ferric Oxide. John Wiley & Sons.
EPA, 2015. 303(d) List Impaired Waters NHDPlus Indexed Dataset with Program Attributes, May 1, 2015 ed. (U.S. Environmental Protection Agency).
Fishman, T., Graedel, T.E., 2019. Impact of the establishment of US offshore wind power on neodymium flows. Nat. Sustain. 2, 332–338.
Foley, N.K., Jaskula, B.W., Kimball, B.A., Schulte, R.F., 2017. Gallium, chapter H of critical mineral resources of the United States - economic and environmental geology and prospects for future supply. U.S. Geol. Surv. Prof. Pap. 1802, H1–H35.
Gambogi, J., 2019a. U.S. Geological Survey, Mineral Commodity Summaries, February 2019, Rare Earths.
Gambogi, J., 2019b. U.S. Geological Survey, Mineral Commodity Summaries, February 2019, Yttrium.
Goonan, T.G., 2014. The lifecycle of silver in the United States in 2009. In: U.S. Geological Survey Scientific Investigations Report 2013-5178, pp. 1–17.
Haque, N., Hughes, A., Lim, S., Vernon, C., 2014. Rare earth elements: overview of mining, mineralogy, uses, sustainability and environmental impact. Resources 3, 614–635.
Hedin, R., Weaver, T., Wolfe, N., Weaver, K., 2010. Passive treatment of acidic coal mine drainage: the Anna S mine passive treatment complex. Mine Water Environ. 29, 165–175.
Hedin, B.C., Capo, R.C., Stewart, B.W., Hedin, R.S., Lopano, C.L., Stuckman, M.Y., 2019. The evaluation of critical rare earth element (REE) enriched treatment solids from coal mine drainage passive treatment systems. Int. J. Coal Geol. 28, 54–64.
Hein, J.R., Mizell, K., Koschinsky, A., Conrad, T.A., 2013. Deep-ocean mineral deposits as a source of critical metals for high- and green-technology applications: Comparison with land-based resources. Ore Geol. Rev. 51, 1–14.
Kairies, C.L., Capo, R.C., Watzlaf, G.R., 2005. Chemical and physical properties of iron hydroxide precipitates associated with passively treated coal mine drainage in the Bituminous Region of Pennsylvania and Maryland. Appl. Geochem. 20, 1445–1460.
Lefticariu, L., Klitzing, K.L., Kolker, A., 2019. Rare Earth Elements and Yttrium (REY) in Coal Mine Drainage from the Illinois Basin. International Journal of Coal Geology, USA.
Lienemann, C.-P., Taillefert, M., Perret, D., Gaillard, J.-F., 1997. Association of cobalt and manganese in aquatic systems: Chemical and microscopic evidence. Geochem. Cosmochim. Acta 16, 1437–1446.
Lifton, J., Hatch, G., 2015. TMR Advanced Rare-Earth Projects Index.
Lin, R., Stuckman, M., Howard, B.H., Bank, T.L., Roth, E.A., Macala, M.K., Lopano, C., Soong, Y., Granite, E.J., 2018. Application of sequential extraction and hydrothermal treatment for characterization and enrichment of rare earth elements from coal fly ash. Fuel 232, 124–133.
Lozano, A., Ayora, C., Fernández-Martínez, A., 2019a. Sorption of rare earth elements onto basaluminite: the role of sulfate and pH. Geochim. Cosmochim. Acta 258, 50–62.
Lozano, A., Fernandez-Martinez, A., Ayora, C., Di Tommaso, D., Poulain, A., Rovezzi, M., Marini, C., 2019b. Solid and aqueous speciation of yttrium in passive remediation systems of acid mine drainage. Environ. Sci. Technol. 53, 11153–11161.
Lozano, A., Ayora, C., Fernández-Martínez, A., 2020. Sorption of rare earth elements on schwertmannite and their mobility in acid mine drainage treatments. Appl. Geochem. 113.
Lynas Corporation Ltd, 2012. Increase in Mt Weld Resource Estimate for the Central Lanthanide Deposit and Duncan Deposit, 56 Pitt Street Sydney NSW 2000.
Moraes, M.L.B., Murciego, A., Álvarez-ayuso, E., Ladeira, A.C.Q., 2020. The role of Al13-polymers in the recovery of rare earth elements from acid mine drainage through pH neutralization. Appl. Geochem. 113.
National Energy Technology Laboratory, 2018. US Department of Energy, Rare Earth Element Database. https://edx.netl.doe.gov/ree/ (accessed on 1 May, 2019).
Noack, C.W., Dzombak, D.A., Karamalidis, A.K., 2014. Rare earth element distributions and trends in natural waters with a focus on groundwater. Environ. Sci. Technol. 48, 4317–4326.
Pu, X., Vazquez, O., Monnell, J.D., Neufeld, R.D., 2010. Speciation of aluminum precipitates from acid rock discharges in Central Pennsylvania. Environ. Eng. Sci. 27, 169–180.
Santelli, C.M., Webb, S.M., Dohnalkova, A.C., Hansel, C.M., 2011. Diversity of Mn oxides produced by Mn(II)-oxidizing fungi. Geochem. Cosmochim. Acta 75, 2762–2776.
Shiel, A.E., Weis, D., Orians, K.J., 2010. Evaluation of zinc, cadmium and lead isotope fractionation during smelting and refining. Sci. Total Environ. 408, 2357–2368.
Silva, G.A., Petter, C.O., Albuquerque, N.R., 2018. Factors and competitiveness analysis in rare earth mining, new methodology: case study from Brazil. Heliyon 4, e00572.
Singer, D.A., Berger, V.I., Moring, B.C., 2008. Porphyry copper deposits of the world: databse and grade and tonnage models. U.S. Geol. Surv. Open-File Rep. 2008-1155, 1–45.
Skousen, J.G., Zipper, C.E., Rose, A., Ziemkiewicz, P.F., Nairn, R.W., McDonald, L.M., Kleinmann, R.L., 2017. Review of passive systems for acid mine drainage treatment. Mine Water Environ. 36, 133–153.
Slack, J.F., Kimball, B.E., Shedd, K.B., 2017. Cobalt, chapter F of critical mineral resources of the United States - Economic and environmental geology and prospects for future supple U.S. Geol. Surv. Prof. Pap. 1802, F1–F40.
Stewart, B.W., Capo, R.C., Hedin, B.C., Hedin, R.S., 2017. Rare earth element resources in coal mine drainage and treatment precipitates in the Appalachian Basin, USA. Int. J. Coal Geol. 169, 28–39.
Stream Restoration, I, 2018. Datashed.
Stuckman, M.Y., Lopano, C.L., Granite, E.J., 2018. Distribution and speciation of rare earth elements in coal combustion by-products via synchrotron microscopy and spectroscopy. Int. J. Coal Geol. 195, 125–138.
Takaya, Y., Yasukawa, K., Kawasaki, T., Fujinaga, K., Ohta, J., Usui, Y., Nakamura, K., Kimura, J.I., Chang, Q., Hamada, M., Dodbiba, G., Nozaki, T., Iijima, K., Morisawa, T., Kuwahara, T., Ishida, Y., Ichimura, T., Kitazume, M., Fujita, T., Kato, Y., 2018. The tremendous potential of deep-sea mud as a source of rare-earth elements. Sci. Rep. 8, 5763.
Tan, H., Zhang, G., Heaney, P.J., Webb, S.M., Burgos, W.D., 2010. Characterization of manganese oxide precipitates from Appalachian coal mine drainage treatment systems. Appl. Geochem. 25, 389–399.
Tanizaki, Y., Shimokawa, T., Yamazaki, M., 1992. Physio-chemical speciation of trace elements in urban streams by size fractionation. Water Res. 26, 55–63.
US Department of the Interior, U.G.S, 2020. Mineral Commodity Summaries, Co. (January 2020).
Van Gosen, B.S., Verplanck, P.L., Seal, R.I.R., Long, K.R., Gambogi, J., 2017. Critical mineral resources of the United States - economic and environmental geology and

prospects for future supply: U.S. Geologic Survey Professional Paper 1802. In: US Department of the Interior, U.G.S. (Ed.), Reston, VA, pp. 1–31.
Vass, C.R., Noble, A., Ziemkiewicz, P.F., 2019a. The occurrence and concentration of rare earth elements in acid mine drainage and treatment by-products: part 1—initial survey of the Northern Appalachian Coal Basin. Min. Metall. Explor. 36, 903–916.
Vass, C.R., Noble, A., Ziemkiewicz, P.F., 2019b. The occurrence and concentration of rare earth elements in acid mine drainage and treatment byproducts. Part 2: Regional survey of Northern and Central Appalachian Coal Basins. Min. Metall. Explor. 36, 917–929.
Verplanck, P.L., Nordstrom, D.K., Taylor, H.E., Kimball, B.A., 2004. Rare earth element partitioning between hydrous ferric oxides and acid mine water during iron oxidation. Appl. Geochem. 19, 1339–1354.
Wallrich, I.L.R., Stewart, B.W., Capo, R.C., Hedin, B.C., Phan, T.T., 2020. Neodymium isotopes track sources of rare earth elements in acidic mine waters. Geochim. Cosmochim. Acta 269, 465–483.
Younger, P.L., Banwart, S.A., Hedin, R.S., 2002. Mine Water: Hydrology, Pollution, Remediation. Kluwer Academic Publishers, Norwell, MA.